

# GradStop: Exploring Training Dynamics in Unsupervised Outlier Detection through Gradient Cohesion

Yuang Zhang      Liping Wang      Yihong Huang      Yuanxing Zheng  
East China Normal University   East China Normal University      Bilibili Inc.      East China Normal University  
Shanghai, China      Shanghai, China      Shanghai, China      Shanghai, China  
51255902045@stu.ecnu.edu.cn   lipingwang@sei.ecnu.edu.cn   hyh957947142@gmail.com   2957573678@qq.com

**Abstract**—Unsupervised Outlier Detection (UOD) is a critical task in data mining and machine learning, aiming to identify instances that significantly deviate from the majority. Without any label, deep UOD methods struggle with the misalignment between the model’s direct optimization goal and the final performance goal of Outlier Detection (OD) task. Through the perspective of training dynamics, this paper proposes an early stopping algorithm to optimize the training of deep UOD models, ensuring they perform optimally in OD rather than overfitting the entire contaminated dataset.

Inspired by UOD mechanism and inlier priority phenomenon, where intuitively models fit inliers more quickly than outliers, we propose GradStop, a sampling-based label-free algorithm to estimate model’s real-time performance during training. First, a sampling method generates two sets: one likely containing more outliers and the other more inliers, then a metric based on gradient cohesion is applied to probe into current training dynamics, which reflects model’s performance on OD task.

Experimental results on 4 deep UOD algorithms and 47 real-world datasets and theoretical proofs demonstrate the effectiveness of our proposed early stopping algorithm in enhancing the performance of deep UOD models. Auto Encoder (AE) enhanced by GradStop achieves better performance than itself, other SOTA UOD methods, and even ensemble AEs. Our method provides a robust and effective solution to the problem of performance degradation during training, enabling deep UOD models to achieve better potential in anomaly detection tasks.

**Index Terms**—Unsupervised Outlier Detection(UOD), Early Stopping, Training Dynamics

## I. INTRODUCTION

### A. Unsupervised Outlier Detection

Outlier Detection (OD) is a fundamental task in data mining and machine learning, focused on identifying instances that significantly deviate from the majority [1], i.e., in our context, inliers. Outliers, usually a minority in the dataset, are alternatively referred to as anomalies, deviants, novelties, or exceptions [1]. OD has received continuous research interests [2]–[4] due to its wide applications in various fields, such as finance [5], security [6], and so on. Depending on the availability of label information, OD methodologies can be classified into three categories: Supervised Outlier Detection, Semi-Supervised Outlier Detection, and Unsupervised Outlier

Detection [7]. Recently, with the development of deep learning, deep OD algorithms are proposed [8]–[10], demonstrating their superior capabilities in managing complex and high-dimensional data types compared to traditional methods.

Unsupervised OD (UOD) targets to detect outliers in a contaminated dataset having both inliers and outliers without the availability of any label [7] by assigning higher anomaly score to outliers. It is important to differentiate between two fundamental paradigms within UOD [11]. The first paradigm, including algorithms such as DeepSVDD [12], NeuTraL AD [13], ICL [14], and AnoGAN [15], is training models exclusively on clean datasets free of outliers. These algorithms subsequently detect potential outliers in unseen test datasets. However, this approach requires the labor-intensive process of collecting large volumes of uncontaminated data before performing outlier detection, thus being less practical.

In contrast, the second category of UOD algorithms including methods like RandNet [16], ROBOD [17], RDP [18], RDA [19], IsolationForest [20], and GAAL [21], is designed to function directly on contaminated datasets that contain outliers. Thus, these models are able to identify outliers within the training set itself and unseen datasets provided that the sample characteristic of the unseen dataset aligns with that of the original training set. Our research focuses on the latter paradigm, where UOD models are trained on datasets that include outliers, presenting a wider use along with more challenges. For both training and validation, no label is available. For clarity, any reference to Unsupervised Outlier Detection throughout the remainder of our work refers to the context of pure unsupervised settings.

### B. Challenge

As widely known, training on contaminated datasets leads to performance degradation or fluctuation. From a UOD perspective, this can also be explained as model misfitting or overfitting to outliers, which is not supposed to happen. In essence, it is caused by the misalignment between the model’s direct optimization goal and the final performance goal of the Outlier Detection task.

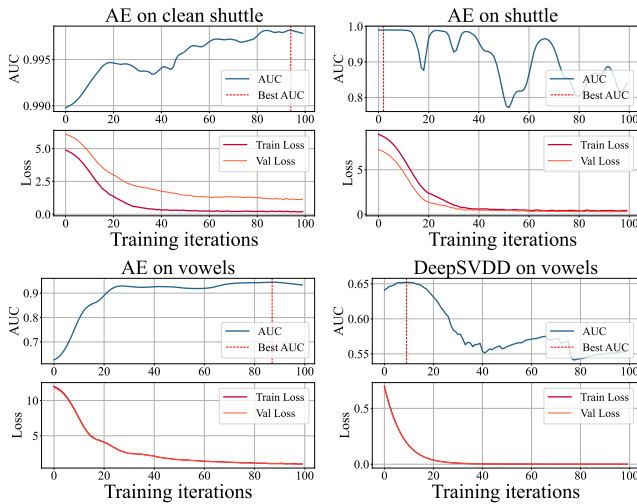


Fig. 1: UOD training process of AutoEncoder and DeepSVDD on datasets *shuttle* and *vowels*.

Due to the unsupervised training setup, Unsupervised Outlier Detection (UOD) can only leverage the distributional differences between outliers and normal instances instead of label information to detect anomalies. For example, outliers usually do not obey specific distributions, include extreme values, have a lower cohesion degree, and are harder to reconstruct. Consequently, UOD models are designed based on outlier assumptions targeting these distributional discrepancies [2]. For instance, AutoEncoder (AE) models assume that outliers are harder to reconstruct. During training, AE minimizes the reconstruction loss and uses reconstruction loss as the anomaly score. This leads to an inherent feature of UOD: the optimization objective of the model is not aligned with the final performance goal of anomaly detection. Therefore, in UOD, performance metrics (such as AUC, AP, etc.) do not necessarily improve strictly with the investment of training resources (e.g., the number of training epochs, model size, etc.).

AE is a typical example. On many datasets including dataset *shuttle* shown in Fig. 1. Outliers from the original dataset *shuttle(contaminated)* are excluded with labels to gain *shuttle(clean)*. On *shuttle(contaminated)*, although the loss value is consistently optimized with training proceeds when training on contaminated datasets, AE’s performance tends to fluctuate or even decline as the number of epochs increases due to the existence of outliers, which is also observed in [11]. By contrast, training on clean datasets (which requires labels) is not subjected to such a problem, as training on *shuttle(clean)*. This phenomenon occurs because, as training progresses, the model begins to reconstruct outliers better, thereby violating the outlier assumption of AE. Although the model becomes better at fitting the overall dataset, outlier detection performance deteriorates. Previous studies have identified this phenomenon and termed it "Inlier Priority" [7] which signifies that the model fits inliers faster and outliers slower. This phenomenon

is a manifestation of the aforementioned outlier assumption during the model training process and also a fundamental mechanism enabling UOD to effectively detect anomalies. Because inliers are easier to fit, there exists a disparity in the degree to which the model fits the inlier distribution versus the outlier distribution at specific stages of training, leading the model to assign higher anomaly scores to outliers. However, as training continues, this disparity diminishes, resulting in a degradation in outlier detection performance.

Current deep UOD approaches lack effective and robust mechanisms to detect and address this performance degradation, keeping deep models from achieving their full potential in outlier detection tasks. Motivated by this, we propose an algorithm to help deep UOD algorithms determine the optimal number of training epochs to prevent degradation, enhancing their performance on the outlier detection task rather than blindly fitting the contaminated dataset. Addressing this challenge involves several challenges:

- **Unsupervised training setup.** Given the fully unsupervised training configuration, a validation set to monitor the model’s real-time performance is unavailable. Instead, we need a label-free yet effective evaluation metric that can infer the model’s OD performance in real-time.
- **Generalization ability on algorithm-dataset pairs.** The outlier assumption is highly dependent on the specific combination of algorithm and dataset. Developing a method broadly applicable across different algorithm-dataset pairs presents a significant challenge. For example, when training AE and DeepSVDD on dataset *vowels* as shown in Fig. 1, the performance of DeepSVDD starts declining since its beginning. Conversely, AE exhibits the opposite behavior with a continuous ascending performance. This variability demands that the proposed algorithm should be capable of identifying optimal training epochs across diverse algorithm-dataset pairs.
- **Complex training dynamics.** The diversity of algorithm-dataset pairs and the associated outlier assumptions can lead to a wide range of training dynamics. Performance during training may exhibit various patterns, such as consistent improvement/decline, initial decline/improvement then improvement/decline, consistent fluctuations, etc. Even in some cases, the UOD algorithm might prove ineffective for the given dataset. The proposed algorithm must be robust enough to handle these diverse and complex training dynamics, ensuring reliable performance across different scenarios.

SOTA UOD studies solve this through overfitting-based ensemble learning [16]–[18], [21]. However, overtraining numerous models brings about large time and computation costs [11]. This paper follows another perspective: to use early stopping to prevent degradation. EntropyStop [11] utilizes a negative probability correlation between AUC and entropy of sample losses to stop the training on AE. However, the entropy metric is small-ranged and sensitive to both algorithm-dataset pair and training dynamics. To meet the challenges, our algorithm aims

to provide an effective, robust, and label-free evaluation metric that can handle various training dynamics of algorithm-dataset pairs. Thus, it optimizes training epochs and maximizes the performance of deep UOD algorithms in OD tasks.

### C. Our Solution

The core idea of the proposed algorithm is also based on the distributional differences between inliers and outliers. As discussed, during training, inlier priority—intuitively, the model more quickly fits inliers while more slowly fits outliers [7]—is one of the typical training dynamics trends exhibited by distributional differences. Specifically, the total contribution of gradient updates from inliers is greater than that from outliers in the early training stage. This phenomenon is the result of a combination of several factors:

- **Gap in quantity and cohesion degree.** Inliers are typically more numerous and exhibit better cohesion, leading to more consistent gradient directions.
- **Inherent difficulty in reconstructing outliers.** Empirically, outliers are inherently harder to reconstruct. At the initialization stage, they often yield larger losses and gradient values.
- **Irregular distribution of outliers.** Outliers tend to obey less predictable distributions, making them harder to fit during training. This irregularity results in poorer gradient cohesion and inconsistent gradient directions.

Consequently, at the beginning of training, the model parameters are more likely to move in the direction that optimizes the inlier gradients, which are more numerous and consistent. As training progresses, outlier gradients contribute more, leading to a dynamic equilibrium where the two balance out. The model parameters then oscillate around the local optima for reconstruction. During the process, model parameters passed but did not stay at a local optima for OD. Therefore, we propose an early stopping algorithm, *GradStop*, to detect such local OD optima and stop the training by monitoring and analyzing training dynamics to solve the challenges. First, a label-free sample method based on outlier assumption generates two sets of data points, each more likely to contain inliers and outliers, respectively. Then a novel metric is applied to the two sets to estimate the inner cohesion degree and inter-divergence degree of in/outlier gradients. Finally, an automated early stopping algorithm determines whether to stop the training at each epoch.

Experiments on 47 real datasets [2] and 4 deep UOD algorithms observed that deep UOD models often achieve high AUC relatively early in training, sometimes even enduring severe degradation since they start training. *GradStop* can effectively solve degradation in many cases and significantly enhances the detection performance of AE and other deep UOD models.

## II. RELATED WORK

### A. Unsupervised Outlier Detection

Unsupervised Outlier Detection (UOD) is a vibrant and rapidly evolving research area focused on identifying outliers

in datasets without labeled data [1]. Traditional methods include Isolation Forest [20], ECOD [22], KNN [23], LOF [24], etc. Recently, deep methods with neural networks have shown advantages in handling large-scale, high-dimensional, and complex data [8]–[10], and have much more potential in generalization on various datasets than traditional methods.

Many deep UOD models [12]–[15] are trained exclusively on clean datasets to learn the distribution of inliers, thus excluding unseen outliers when testing. However, real-world datasets are usually large and may inadvertently contain outliers that the model should detect [25]. To address this issue, studies [18], [19], [26] have focused on algorithms that train directly on contaminated datasets, where the misalignment of optimization goal exists.

Efforts have been made to mitigate the model degradation caused by the misalignment. Model ensemble approaches [16], [17], [21] are proposed with better performance and robustness against hyperparameters (HPs). Additionally, [25], [27], [28] adapt models initially trained on clean datasets to perform effectively on contaminated datasets through outlier refinement processes.

### B. Early Stopping

Early stopping is an effective and widely employed technique in machine learning, designed to halt training when further iterations no longer benefit the final performance. One of the well-known applications of early stopping is its use as a regularization method to mitigate overfitting, often in conjunction with cross-validation [29]. More recently, a deeper understanding of training dynamics has revealed the practical utility of early stopping in scenarios involving noisy labels [30]–[33]. These studies indicate that overfitting to noisy samples in the later stages of training can degrade model performance, an issue that can be alleviated through early stopping. Previous research has demonstrated the remarkable ability of early stopping to handle noisy learning environments. [11] is the first to explore the potential of early stopping in UOD with loss entropy as the stopping metric, demonstrating the rationality and effectiveness of early stopping in UOD to solve model degradation problems. However, the metric is sensitive to algorithm-dataset pair and training dynamics. Our work further delves into the path of early stopping UOD, proposing a more robust and generalizable evaluation metric.

## III. PRELIMINARY

**Problem Formulation** (Unsupervised OD). *Considering a data space  $\mathcal{X}$ , an unlabeled dataset  $\mathcal{D} = \{\mathbf{x}_j\}_{j=1}^n$  consists of an inlier set  $\mathcal{D}_{in}$  and an outlier set  $\mathcal{D}_{out}$ , which originate from two different underlying distributions  $\mathcal{X}_{in}$  and  $\mathcal{X}_{out}$ , respectively [34]. The goal is to learn an outlier score function  $f(\cdot)$  to calculate the outlier score value  $v_j = f(\mathbf{x}_j)$  for each data point  $\mathbf{x}_j \in \mathcal{D}$ . Without loss of generality, a higher  $f(\mathbf{x}_j)$  indicates more likelihood of  $\mathbf{x}_j$  to be an outlier.*

**Unsupervised Training Formulation for OD.** Given a UOD model  $M$ , at each iteration, a batch of instances  $B =$

$\{x_0, x_1, \dots, x_n\}$  is sampled from the data space  $\mathcal{X}$ . The loss  $\mathcal{L}$  for model  $M$  is calculated over  $B$  as follows:

$$\mathcal{L}(M; B) = \frac{1}{|B|} \sum_{x \in B} \mathcal{J}_M(x) = \frac{1}{|B|} \sum_{x \in B} f_M(x) = \frac{1}{|B|} \sum_i v_i \quad (1)$$

where  $\mathcal{J}_M(\cdot)$  denotes the unsupervised loss function of  $M$  while  $\mathcal{L}$  denotes the loss based on which the model  $M$  updates its parameters by minimizing  $\mathcal{L}$ , with assumption that the learning rate  $\eta$  is sufficiently small. To facilitate understanding, we assume here the unsupervised loss function  $\mathcal{J}_M(\cdot)$  and outlier score function  $f_M(\cdot)$  are identical.

**Objective:** The objective is to train the model  $M$  such that it achieves the best detection performance on  $\mathcal{X}$ . Specifically, we aim to maximize the probability that an inlier from  $\mathcal{X}_{in}$  has a lower outlier score than an outlier from  $\mathcal{X}_{out}$ , i.e.,

$$P(v^- < v^+) = P(f_M < f_M(x_{out}) | x_{in} \sim \mathcal{X}_{in}, x_{out} \sim \mathcal{X}_{out}) \quad (2)$$

as large as possible, where  $f_M(\cdot)$  is the outlier score function learned by model  $M$ . Let  $\mathcal{O}_{in}$  and  $\mathcal{O}_{out}$  represent the distributions of  $f_M(x)$ , where  $x$  is drawn from  $\mathcal{X}_{in}$  and  $\mathcal{X}_{out}$ , respectively. Therefore,  $v^- \sim \mathcal{O}_{in}$  and  $v^+ \sim \mathcal{O}_{out}$  denotes the corresponding random variable of outlier score.

**The relationship between  $P(v^- < v^+)$  and AUC .** AUC [35] is a widely-used metric to evaluate the outlier detection performance, which can be formulated as:

$$AUC(M, \mathcal{D}) = \frac{1}{|\mathcal{D}_{in}| |\mathcal{D}_{out}|} \sum_{\mathbf{x}_i \in \mathcal{D}_{in}} \sum_{\mathbf{x}_j \in \mathcal{D}_{out}} \mathbb{I}(f_M(\mathbf{x}_i) < f_M(\mathbf{x}_j)) \quad (3)$$

where  $\mathbb{I}$  is an indicator function. In practice, AUC is discretely computed on a dataset, and the expression  $P(v^- < v^+)$  is the continuous form of AUC.  $P(v^- < v^+)$  signifies the model's inherent capability to distinguish between inliers and outliers from a view of the data distribution instead of a certain dataset.

#### IV. METHODOLOGY

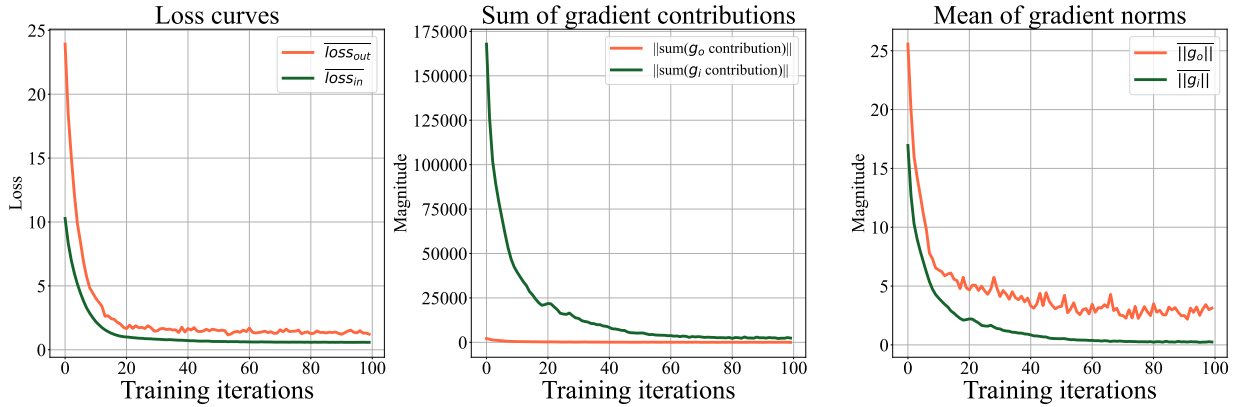
In this section, we elucidate the methodology of the proposed early stopping method, **GradStop**. In the beginning, we explain the connection between training dynamics and the final outlier detection goal from both intuitive and theoretical perspectives, showing its fundamental mechanism. Subsequently, we introduce a gradient-based sample method that can generate two small sets of training samples—one is more likely to contain inliers and the other outliers—without any label. Then, a gradient-based metric is calculated upon the two sets to evaluate their inner cohesion and inter-divergence, reflecting the model's OD performance. Finally, we introduce GradStop by utilizing the automated early stopping algorithm similar to [11] with our novel sample method and metric.

##### A. Connection between Training Dynamics and Outlier Detection Goal

As previously mentioned, there is a misalignment between the model's optimization goal and the OD goal in UOD. The OD goal is grounded in outlier assumptions, which can be reflected through training dynamics such as inlier priority during the training process. Therefore, by analyzing training dynamics, one can infer whether the algorithm's underlying outlier assumptions are satisfied under the current model parameters.

Next, we will combine examples to detailedly explain the relationship between outlier assumptions and training dynamics. A widely used and effective outlier assumption in UOD is the reconstruction assumption, which posits that outliers are harder for the model to reconstruct during training. An illustrative example is shown in Fig. 2 describing training dynamics of AE training on dataset *cover*. The upper right and lower plots witness that the mean of the outlier loss distribution is consistently larger than that of the inlier, aligning with the outlier assumption. This assumption holds in most OD conditions fundamentally due to the differences in normal and abnormal data distribution, including the gap in quantity and cohesion degree, inherent difficulty in reconstructing outliers, and irregular distribution of outliers. First, inliers typically usually follow a regular distribution and far outnumber outliers. In the case of *cover*, outliers only take up 0.96% of the overall dataset. This makes the model utilize far more gradients from inlier values than those from outliers during parameter updates, with inlier gradients exhibiting stronger cohesion and more consistent direction. As a result, the total gradient magnitude for inlier values is often larger, which can be empirically verified in the middle plot of Fig. 2a. The contributions are gained by calculating the projection of summed in/outlier gradients on the direction of the overall gradient update in each epoch [36]. At the early stages of training AE on *cover*, inliers almost dominate the parameter updates. However, experiments also show that the average gradient magnitude of outliers often significantly exceeds that of inliers during the whole training process, shown in the right plot of Fig. 2a. This phenomenon is due to, first, the inherent difficulty in reconstructing outliers; second, outliers less frequently obey a specific, regular distribution, leading to their gradients being less cohesive, less aligned directionally, and thus counteract each other, making it harder for the model to fit (thus reduce) them during training. Similar training dynamics are also observed in learning in class imbalance environments [36]. Since OD can also be viewed as a two-class classification task with two classes severely imbalanced [37], these training dynamics occur reasonably.

Therefore, on the individual gradient level, the initial values of outliers are often larger; on the whole distribution level, outliers are more difficult to fit during training. Thus, heuristically, throughout the entire training process, from model initialization to the final local optimum where in/outliers gradients push and pull the model parameters, the individual



(a) The curves from left to right represent: the average in/outlier loss values, the magnitude of the sum of in/outlier gradient contributions in the corresponding epoch’s gradient update, and the average in/outlier gradient magnitudes.

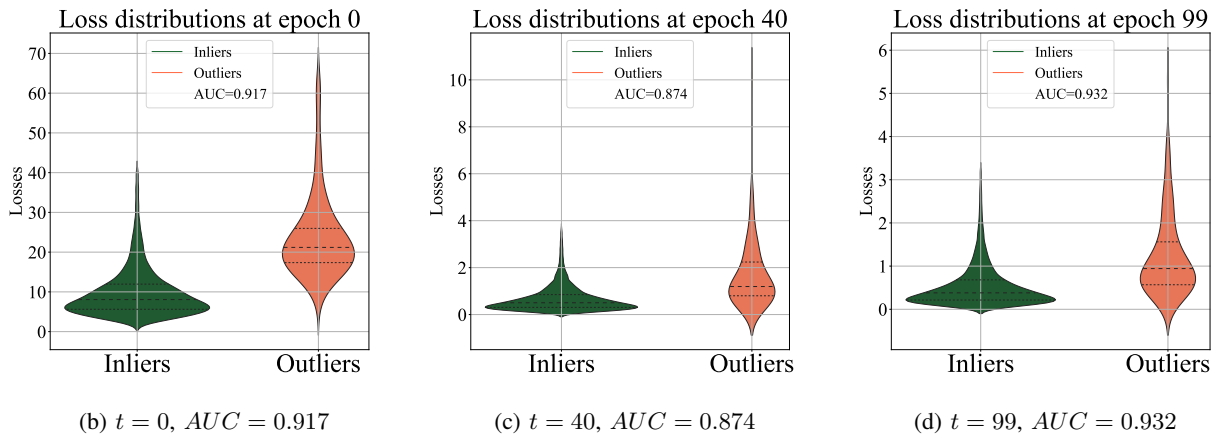


Fig. 2: Training dynamics of AE training on dataset *cover*, in which outlier proportion is 0.96%. Dark green denotes the inliers, and orange denotes the outliers.

gradients of outliers remain larger than those of inliers, as shown in the right plot of Fig. 2a.

Furthermore, we theoretically demonstrate the relationship between inlier priority, a crucial outlier assumption for the OD task, and the training dynamics. Specifically, when the cohesion of the sample gradients of inliers and outliers meets certain conditions, we can derive a lower bound for the difference in the rate of loss decrease between inliers and outliers. This ensures the occurrence of inlier priority, thus ensuring the effectiveness of the OD task.

The theoretical analysis in Subsection VII-B provides a solid foundation for understanding how and why inlier priority, which is essential for the effectiveness of the OD task, can be maintained during the training process and observed with training dynamics. It also supports the practical utility of the following metrics and methods proposed in our GradStop algorithm. Here we only bring up Theorem 1:

**Theorem 1.** *With certain assumptions and  $r_t > \cos \theta_t R + \sqrt{\cos^2 \theta_t R^2 + 2R + 1}$ , we have loss decreasing speed gap  $\hat{\Delta}_t^f > 0$ , which means inlier priority strengthens at epoch  $t$ .*

For the details of the assumptions, notations, and further explanation, please refer to Subsection VII-B.

### B. Gradient-based sample method GradSample

In this subsection, we propose a simple yet effective sampling method **GradSample** as part of the GradStop algorithm. GradStop involves sampling two small sets of size  $k$  from the training data points in each training epoch, where the samples are respectively more likely to be inliers and outliers, without any label. As stated, throughout the entire training process, the individual gradients of outliers are larger than those of inliers. Therefore, during each gradient update, the gradients of the samples participating in the update are extracted to calculate their magnitudes, and  $k$  gradient vectors with the greatest and least magnitudes are selected to form two sets,  $G_i^{\text{top}}$  and  $G_i^{\text{last}}$ , where  $i$  denotes the epoch number. Consequently, each data point corresponding to a gradient vector in  $G_i^{\text{top}}$  has a higher probability of being an outlier, and vice versa. Given the model at  $t$ -th epoch  $M_t$ , dataset  $\mathcal{D}$  and sample number  $k$ , we have:

$$G_t^{\text{top}}, G_t^{\text{last}} = \mathbf{GradSample}(M_t, \mathcal{D}, k) \quad (5)$$

**GradSample**( $M_t, \mathcal{D}, k$ ) standing for gradient-sample is detailed in Algorithm 1.

### C. Gradient-based Metric: Cohesion and Divergence

With these two sets,  $G_t^{\text{top}}$  and  $G_t^{\text{last}}$ , we can gain insights into the current training dynamics of the model by analyzing them, to check whether it still aligns with the outlier assumptions. Since the sets do not strictly reflect the ground-truth labels, we cannot compute based on labels for each gradient vector; however, because they exhibit tendencies similar to inliers and outliers on a collective level, we can adopt statistical measures such as mean or variance that reflect the overall characteristics of them. Furthermore, these metrics should be capable of reflecting the outlier assumptions. Therefore, we have designed two metrics to respectively reflect the **inner cohesion** and **inter-divergence** of the inlier and outlier classes. These are determined based on the distribution assumptions of inliers and outliers: the gradients of inliers exhibit better inner cohesion, thereby facilitating better learning of normal values. Effective parameter updates during computation should demonstrate this, proving that the model can effectively exhibit inlier priority to accomplish the OD task. Also, the overall gradient direction of inliers and outliers can reflect the features currently learned by the model: if the directions are relatively consistent, it indicates that the model is learning the similarity of inliers and outliers; if the directions are relatively inconsistent, it suggests that the loss of inliers and outliers cannot be reduced simultaneously, indicating that the model has already learned the similarities. The former often occurs during the early stage of training, accompanied by inlier priority strongly holds; the latter is on the contrary, usually with inliers maximally learned or at an oscillation phase. The contribution to the OD task is much smaller in the latter phase compared to the former.

Given a set of gradient vectors  $G = \{g_1, \dots, g_k\}$ , the cohesion metric  $\mathbf{C}$  is defined in equation 6.

$$\mathbf{C}(G) = \frac{\|\sum_1^k g_i\|}{\sum_1^k \|g_i\|} \in [0, 1] \quad (6)$$

To understand the metric, when all vectors in  $G$  completely counteract each other,  $\mathbf{C}(G)$  equals to 0; when all vectors in  $G$  are in the same direction,  $\mathbf{C}(G)$  equals to 1.

Given two sets of gradient vectors  $G^1 = \{g_1^1, \dots, g_k^1\}$  and  $G^2 = \{g_1^2, \dots, g_k^2\}$ . The divergence metric  $\mathbf{D}$  is defined in equation 7.

$$\mathbf{D}(G_{\text{top}}, G_{\text{last}}) = \theta_t = \angle(\sum_1^k g_i^1, \sum_1^k g_i^2) \quad (7)$$

in which  $\angle(u, v)$  means the angle value between vectors  $u$  and  $v$ .  $\mathbf{C}$  and  $\mathbf{D}$  are also associated with the theoretical proof in Subsection VII-B.

### D. GradStop: Automated Early Stopping Algorithm

Thus, we have developed metrics to measure inner cohesion and inter-divergence between inliers and outliers, along with the outlier assumptions related to these metrics, which are closely associated with the Outlier Detection (OD) task. Based

on these two metrics, we design *GradStop*, an early stopping algorithm that can dynamically assess whether the current training state of the model aligns with the outlier assumptions through the lens of training dynamics. If not, it is inferred that the model has reached or is nearing its optimal performance on the OD task, and training should be halted to prevent toxic training caused by goal misalignment. The algorithm is detailed in 1.

---

#### Algorithm 1: GradStop: An early stopping algorithm for deep UOD model based on training dynamics

---

**Input:** Model  $M$  with learnable parameters  $\Theta$ , downtrend threshold  $R_{\text{down}}$ , dataset  $\mathcal{D}$ , iterations  $T$ , sampling number  $k$ , evaluation batch number  $n$ , sliding window size  $w$

**Output:** Outlier score list  $\mathbf{O}$

- 1 Initialize the parameter  $\Theta_1$  of Model  $M_1$ ;
- 2 Random sample  $n$  instances from  $\mathcal{D}$  as the evaluation batch  $B_{\text{eval}}$ ;
- 3  $\Theta_{\text{best}} \leftarrow \Theta_1$ ;  $H \leftarrow 0$ ;      /\* Model Training \*/
- 4 **for**  $t := 1 \rightarrow T$  **do**
- 5      $\mathcal{L}_t = f(\Theta_t, \mathcal{D})$ ;
- 6     Optimize  $\Theta_t$  by optimizer( $\Theta_t, \mathcal{L}_t$ ) by minimizing  $\mathcal{L}_t$ ;
- 7      $G_t^{\text{top}}, G_t^{\text{last}} = \mathbf{GradSample}(M_t, B_{\text{eval}}, k)$ ;
- 8      $C^{\text{diff}}[t] \leftarrow C(G_t^{\text{last}}) - C(G_t^{\text{top}})$ ;
- 9      $\mathbf{D}[t] = \mathbf{D}(G_t^{\text{top}}, G_t^{\text{last}})$ ;
- 10     $H \leftarrow H + (C^{\text{diff}}[t] - C^{\text{diff}}[t-1])$ ;
- 11    **if**  $(C^{\text{diff}}[t] \geq \max(C^{\text{diff}}[t-w+1:t])$  and  $\frac{1}{H}(C^{\text{diff}}[t] - \max(C^{\text{diff}}[t-w+1:t]) > R_{\text{down}})$  or  $(C^{\text{diff}}[t] > t_{\text{cb}}$  or  $|C^{\text{diff}}[t]| < t_{\text{cs}})$  **then**
- 12        $\Theta_{\text{best}} \leftarrow \Theta_t$ ;
- 13    **end**
- 14    **else**
- 15       **if**  $C^{\text{diff}}[t-w] \geq \max(C^{\text{diff}}[t-w+1:t])$  **then**
- 16            Break;
- 17       **end**
- 18    **end**
- 19 **end**
- 20 **if**  $\mathbf{D}[:w] < t_{\text{D}}$  **then**
- 21    Load  $\Theta_{\text{best}}$  to  $M$ ;
- 22 **end**
- 23 **else**
- 24    Load  $\Theta_1$  to  $M$ ;
- 25 **end**
- Return:**  $\{f_M(x), x \in \mathcal{D}\}$

---

We follow the one proposed in [11] for determining stopping except for an additional sliding window mechanism. Window size  $w$  is similar to the patience parameter for searching the optimal iteration in [11], and  $R_{\text{down}}$  sets the requirement for the smooth degree of downtrend. A larger  $w$  usually improves accuracy at the expense of longer training time. Generally, GradStop does the following two things:

- At the early stage of training, check if  $\mathbf{D}(G_{\text{top}}, G_{\text{last}}) > t_{\text{D}}$  is continuously satisfied, if so, choose the initial model parameter. This suggests that inliers and outliers are inherently distinguished by the model with its structure, and probably learning mechanism is completely useless for certain algorithm-dataset pairs. In this circumstance,

**Algorithm 2:** GradSample: An sampling algorithm based on training dynamics when training deep UOD model

---

**Input:** Model  $M_t$  with learnable parameters  $\Theta_t$ , evaluation set  $B_{eval} = \{x_1, \dots, x_n\}$ , sampling number  $k$

**Output:** Two sets of gradient vectors,  $G_t^{top}, G_t^{last}$

- 1 Calculate  $G = \{g_i \mid x_i \in B_{eval}\}$  with  $g_i$  being the gradient vector of  $M_t(x_i)$ ;
- 2 Calculate  $G_{norm} = \{\|g_i\| \mid g_i \in G\}$ ;
- 3  $i_{top} = \text{argsort}(G_{norm})[1 : k]$ ;
- 4  $i_{last} = \text{argsort}(G_{norm})[n - k + 1 : n]$ ; /\* argsort( $l$ ) returns indices of list  $l$  in value-ascending order. \*/
- 5  $G^{top} = G[i_{top}]$ ;
- 6  $G^{last} = G[i_{last}]$ ;

**Return:**  $G^{top}, G^{last}$

---

performance will consistently degrade. The random initialized model may exhibit the best performance. This phenomenon is empirically observed when training AE and DeepSVDD on a number of datasets, as training DeepSVDD on *vowels* shown in Fig.1

- At every training epoch, calculate  $C_{\Delta} = C(G_{top}) - C(G_{last})$ . If it is smaller than a benefit threshold  $t_{Cb}$  and has not been increasing for  $w$  epochs, indicating a useless learning is going on, halt the training. Additionally,  $|C^{diff}[t]|$  should be larger than a significance threshold  $t_{Cs}$  to stop training, which assures that the model would not stop training when there is no significant difference between  $C(G_{top})$  and  $C(G_{last})$ , which usually happens when current model parameter is unable to distinguish inliers and outliers effectively.

With GradStop, we can terminate training when the outlier assumptions no longer hold and select the epoch that the training dynamics best conform to the outlier assumptions as the final model output, improving the model’s final performance on the OD task.

## V. EXPERIMENTS

The experiment consists of three parts: experiment settings, GradAE performance, and improvements on Other Deep UOD Models. In GradAE performance, we apply GradStop to the AutoEncoder (AE) model, a widely used deep UOD method, to gain GradAE, achieving comparable performance with other SOTA UOD baselines. Then, improvements on other deep UOD Models are evaluated to show the generalization ability and robustness of GradStop.

### A. Experiment Settings

All experiments adopt a transductive setting, where the training set equals the test set, which is common in Unsupervised OD [16], [17].

#### 1) Dataset

Experiments are carried out on 47 widely-used real-world tabular datasets<sup>1</sup> collected by [2], which cover many applica-

TABLE I: Real-world dataset pool

	Dataset	Num Pts	Dim	% Outlier
1	ALOI	49534	27	3.04
2	anthroid	7200	6	7.42
3	backdoor	95329	196	2.44
4	breastw	683	9	34.99
5	campaign	41188	62	11.27
6	cardio	1831	21	9.61
7	Cardiotocography	2114	21	22.04
8	celeba	202599	39	2.24
9	census	299285	500	6.20
10	cover	286048	10	0.96
11	donors	619326	10	5.93
12	fault	1941	27	34.67
13	fraud	284807	29	0.17
14	glass	214	7	4.21
15	Hepatitis	80	19	16.25
...	...	...	...	...
...	...	...	...	...
43	WDBC	367	30	2.72
44	Wilt	4819	5	5.33
45	wine	129	13	7.75
46	WPBC	198	33	23.74
47	yeast	1484	8	34.16

tion domains, including healthcare, image processing, finance, etc. The information of the 47 datasets is shown in Table I.

#### 2) Evaluation Metrics

We evaluate performance with AUC, a widely used evaluation metric in the field of OD, defined in Equation 4. Computing AUC does not need any threshold for outlier scores outputted by the model, as they are ranking-based metrics.

#### 3) Computing Infrastructures

All experiments are conducted on 12th Gen Intel(R) Core(TM) i5-12400F CPU, and NVIDIA GeForce RTX 3060 Ti (8GB GPU memory) GPU, CUDA Version 12.2.

### B. GradAE Performance Study

We first study how much improvement can be achieved by employing GradStop on AE model. VanillaAE denotes the simplest form of AE without any additional technique, with only one hidden layer with size  $h_{dim} = 64$ . We apply our early stopping method to VanillaAE to gain **GradAE**. Then, GradAE is compared with two ensemble AEs, the recent SOTA hyper-ensemble ROBOD [17] and the widely-used RandNet [16]. The experiments of two ensemble models are based on the open-source code of ROBOD<sup>2</sup>. We also choose EntropyAE with EntropyStop [11] as one of the baselines, since it is the pioneering work applying early stopping to deep UOD. EntropyStop is an early stopping algorithm for deep UOD models, which stops training and chooses the model parameter with the lowest loss entropy in past epochs as the final result. Another family of UOD is traditional methods including IF [20], ECOD [22], KNN [23], CBLOF [38] and GMM [26]. Compared to deep methods, traditional methods may lack some potential for generalization and the ability to deal with

<sup>1</sup><https://github.com/Minqi824/ADBench/>

<sup>2</sup><https://github.com/xyvivan/ROBOD>

TABLE II: Detection performance of models from AE family and other SOTA UOD methods.

Family of AE models					
	VanillaAE	GradAE (Ours)	EntropyAE	RandNet	ROBOD
$\overline{AUC}$	0.758±0.004	<b>0.775±0.003</b>	0.768±0.005	& 0.728±0.00	0.736±0.00
$\overline{Rank}_{AUC}$	6.617	<b>4.875</b>	4.896	6.042	5.792
Traditional UOD methods					
	Isolation Forest	ECOD	KNN	CBLOF	GMM
$\overline{AUC}$	0.764±0.00	0.742±0.00	0.720±0.00	0.748±0.00	0.758±0.00
$\overline{Rank}_{AUC}$	5.000	5.771	5.792	5.167	5.417

high-dimensional data, but still, they are very competitive in UOD and perform well on certain datasets.

### 1) Detection Performance Result on AE

The average result of three runs is reported in Table II. Experiment details can be found in VII-D. We conducted a comparative analysis of four UOD methods across 47 datasets, evaluating average AUC, and average ranking in AUC. GradAE not only significantly outperforms VanillaAE but also gains superior performance over ensemble models. For each dataset, we ranked the AUC performance of the ten algorithms and listed the average ranking of each algorithm across all datasets in the table. In terms of AUC, GradStop improved VanillaAE’s score from 0.758 to 0.775, an increase of approximately 2.24%. Moreover, GradAE achieved a ranking of 4.875, surpassing the second-place EntropyAE’s 4.896 and significantly outperforming VanillaAE’s 6.617. By employing early stopping, GradAE effectively mitigates the problem of goal misalignment when training AutoEncoder, thus improving the overall performance of VanillaAE.

### C. Improvements on other Deep UOD Models

In this subsection, we apply GradStop to other Deep UOD models, including VAE [39], DeepSVDD [12], and RDP [18], to validate the generalization capability of the GradStop algorithm across multiple algorithm-dataset pairs and its robustness against complex training dynamics. Both VAE and DeepSVDD aim to optimize the model’s reconstruction loss. In contrast, RDP trains the model to learn and predict the sample distances of a random projection network as its optimization goal. Experiments show that GradStop significantly enhances the performance of unsupervised DeepSVDD, followed by RDP, with VAE showing the least improvement. Implementations of DeepSVDD and VAE are from PyOD<sup>3</sup>, and implementation of RDP is from [18]<sup>4</sup>. Then, we discuss the overall results of all four models including AE.

### 1) Detection Performance Result on deep UOD models

The overall result of the experiment is in table III, listing 6 models, DeepSVDD, RDP, and VAE along with their GradStop and EntropyStop [11] versions. "Num. Datasets" denotes the number of datasets on which the model performs better than its corresponding vanilla version or GradStop version among all 47 datasets. The patience parameter of EntropyStop and

the window size of GradStop are both set to 20 and  $R_{down}$  are both 0.001.

From III, we can see that GradStop significantly improves DeepSVDD, increasing its AUC from 0.502 to 0.648, an improvement of 29.08%, and enhancing performance on a majority 38 out of 47 of the datasets. In contrast, the improvements on RDP and VAE are smaller, with RDP’s AUC increasing from 0.742 to 0.747, and VAE’s AUC from 0.746 to 0.747; performance only on 22 (RDP) and 17 (VAE) out of 47 datasets are improved. Additionally, compared to EntropyStop, GradStop performs better on all four deep UOD models (including AE), demonstrating its stronger generalization ability across different algorithm-dataset pairs and robustness to complex training dynamics.

### 2) Discussions

The performance improvement of the GradStop algorithm on deep UOD models decreases in the order of DeepSVDD, AE, RDP, and VAE. Following we briefly analyze the reasons.

First, AE is the simplest and generally the best-performing model. Its optimization goal is reconstruction loss, which can be affected by goal misalignment, leading to trends of AUC rising, falling, or fluctuating across different datasets. AUC decreases when AE fits better to outliers. GradStop can detect this phenomenon and halt training, thus providing a performance boost for AE.

DeepSVDD is more susceptible to the impact of outliers compared to AE, making it more prone to goal misalignment and performance degradation. This is due to its optimization goal, which minimizes the hypersphere radius in the latent space that encloses all data point representations. As a result, the quantitative advantage of inliers is partly weakened, and the model is more likely to learn outliers far from the center of the hypersphere.

On the other hand, VAE and RDP impose the strongest constraints on the latent space. VAE enforces a regularization constraint to make the latent variables follow a normal distribution, while RDP specifies an additional distance function and requires the distance space of the latent vectors to fit a randomly projected distance space. These constraints help mitigate the problem of goal misalignment since the distribution pattern of representations is fixed, thus reducing the benefits of early stopping. However, these constraints also limit the model’s representation capacity, making it harder for the model to flexibly fit complex inliers, leading to a performance lower than AE, which imposes no constraints on the representation space.

## VI. CONCLUSION

In the context of deep Unsupervised Outlier Detection (UOD), there exists an inherent misalignment between the model optimization goal and the goal of the UOD task due to the lack of label guidance. In this work, inspired by the characteristics of outlier distributions and inlier priority [7], we elucidate the connection between the UOD goal, outlier assumptions, and UOD training dynamics. Then we propose a label-free gradient-based sampling method, *GradSample*, to

<sup>3</sup><https://github.com/yzhao062/pyod>

<sup>4</sup><https://github.com/billhhh/RDP>



TABLE III: Detection performance of deep UOD models and their GradStop and EntropyStop versions (with respectively -G and -E suffix in the model name). "Num. Datasets" denotes the number of datasets on which the model performs better than its counterpart among all 47 datasets. Patience parameters are set to 20.

	Models				Improvements
	DeepSVDD	DeepSVDD-G	DeepSVDD-E	DeepSVDD-G	
AUC	0.502	<b>0.648</b>	0.51		<b>29.08%</b>
Num. Datasets	9	38	—		<b>80.85%</b>
	RDP	RDP-G	RDP-E	RDP-G	
AUC	0.742	<b>0.747</b>	0.744		0.67%
Num. Datasets	25	22	—		46.81%
	VAE	VAE-G	VAE-E	VAE-G	
AUC	0.746	0.747	0.746		0.13%
Num. Datasets	30	17	—		36.17%

generate two sets that are more likely to contain inliers and outliers, respectively. Two metrics, inner cohesion and inter-divergence, are designed to measure the outlier assumptions during training. With an additional early stopping technique [11], **GradStop** can halt training before the outlier assumptions of deep UOD models are violated, selecting the optimal training epoch to help the model reach its potential. Experimental results show that applying GradStop on AutoEncoder can significantly enhance its performance, surpassing existing SOTA UOD baselines. Furthermore, GradStop is applicable to different algorithm-dataset pairs and handling various training dynamics. Experiments on DeepSVDD, VAE, and RDP indicate that it can improve the performance of current deep UOD models and effectively mitigate the issue of goal misalignment.

Future work involves further exploring the potential and application of training dynamics, especially in unsupervised scenarios where label guidance is unavailable. For example, GradSample might be used to generate pseudo labels that could transform unsupervised learning into weakly supervised learning, combined with loss functions from a distributional view such as [40]. Additionally, the current approach treats the metrics as auxiliary indicators for early stopping. A better approach might be to integrate them into the optimization goal rather than as an additional auxiliary early-stopping metric. Moreover, the proposed metrics are ineffective in some cases across the 47 datasets. Further exploration of training dynamics in these scenarios and conducting more in-depth analysis and explanation can help us better understand the deep UOD training mechanism and design solution algorithms.

## VII. SUPPLEMENTARY DETAILS

### A. Notations

We summarize the notations of GradStop algorithm here. For clarity, we simplified the notations in a full batch gradient descent setting. At any epoch  $t$ , we denote current training dynamics as:

- $t$ : time, i.e., the number of training epoch.
- $\mathcal{D}$ : the training dataset.

- $M$ : a UOD model.  $M_t$  denotes model at epoch  $t$ .
- $k$ : the number of data points when performing  $top-k$  and  $last-k$  sampling in GradSample.
- $B_{eval} = \{x_1, \dots, x_n\}$ : the evaluation batch on which we perform GradStop.
- $G = G_{B_{eval}} = \{g_1, \dots, g_n\}$ : a set of gradient vectors generated by model  $M_t$  on  $B_{eval}$ . Usually,  $n$  equals to evaluation batch size  $\|B_{eval}\|$  with  $g_i$ 's dimensionality equals to the dimensionality of parameter space  $\|M\|$ .
- $G_{top}, G_{last}$ : sets of gradient vectors generated by GradSample on  $G$ .
- $\mathbf{C}(G_{top}), \mathbf{C}(G_{last})$ : the cohesion metric reflecting the cohesion degree of gradient set  $G_{top}$  or  $G_{last}$ .
- $\mathbf{D}(G_{top}, G_{last})$ : the divergence metric reflecting the divergence degree between gradient set  $G_{top}$  and  $G_{last}$ .
- $t_{Cs}, t_{Cb}$ : the significance threshold and benefit threshold of cohesion metric, with  $t_{Cs} < t_{Cb}$ .
- $t_D$ : the stopping threshold of divergence metric.
- $w$ : the size of the sliding window of the early stopping algorithm.
- $R_{down}$ : the smooth parameter in stopping algorithm by [11].

### B. Theoretical Demonstration of Inlier Priority

The related notations in our proof are as follows.

- $\mathcal{D}$ : the training dataset.
- $|C_i|, |C_o|$ : the number of samples belonging to inliers and outliers, respectively.
- $R = \frac{|C_i|}{|C_o|}$ : the ratio of the number of inliers to the number of outliers.
- $L$ : Lipschitz constant, with regard to Lipschitz smooth.
- $t$ : time of the training process (i.e., number of iterations).

At each time  $t$ , we have:

- $\eta_t$ : learning rate, a positive real number.
- $\omega_t$ : set of network parameters.
- $f(\omega_t) = \sum_{x \in \mathcal{D}} f_x(\omega_t)$ : loss function summed over all samples in the dataset.
- $f^i(\omega_t) = \sum_{x \in C_i} f_x(\omega_t)$ : loss function summed over all samples belonging to inliers. Similarly, we have  $f^o(\omega_t) = \sum_{x \in C_o} f_x(\omega_t)$
- $\nabla f^i(\omega_t)$ : gradient computed on the loss function summed over all samples belonging to inliers. Similarly, we have  $\nabla f^o(\omega_t)$ .
- $\theta_t$ : the angle between  $\nabla f^i(\omega_t)$  and  $\nabla f^o(\omega_t)$ .
- $\nabla f(\omega_t) = \nabla f^i(\omega_t) + \nabla f^o(\omega_t)$ : gradient computed on the loss function summed over all samples.
- $\nabla_i = \|\nabla f^i(\omega_t)\|$ : the norm of the overall gradient of inliers. For clarity,  $t$  is omitted in the simplified notation  $\nabla_i$  in some formulas.
- $r_t = \frac{\nabla_i}{\nabla_o}$ : the ratio of the norms of the inlier gradients to outlier gradients.
- $\Delta_t^f = (f^i(\omega_t) - f^i(\omega_{t+1})) - (f^o(\omega_t) - f^o(\omega_{t+1}))$ : the difference of the decreasing speed of summed loss value between two classes.
- $\hat{\Delta}_t^f = \frac{1}{|C_i|}(f^i(\omega_t) - f^i(\omega_{t+1})) - \frac{1}{|C_o|}(f^o(\omega_t) - f^o(\omega_{t+1}))$ : *loss decreasing speed gap*, the difference of the de-

creasing speed of averaged loss value between inliers and outliers. If  $\tilde{\Delta}_t^f > 0$ , **inlier priority strengthens**.

### 1) Derivation of the range

The main purpose of the proof is to demonstrate the connection between inlier priority, a crucial outlier assumption for the OD tasks, and certain training dynamics. Then, we can utilize these dynamics to monitor whether inlier priority is strengthening or weakening, and infer OD performance.

First, we would like to recap inlier priority and its importance. In outlier detection scenarios, the decreasing speed of the averaged loss value of inliers differs from one of the outliers due to their different distribution. To be specific, initially, average inlier reconstruction loss decreases rapidly, while average outlier loss decreases rather slowly, generating a huge gap between the two average losses after a short period. This gap is utilized by current OD methods to distinguish outliers. However, with the proceeding of learning, the gap is gradually mended, since both losses converge to 0. The aforementioned OD methods will fail after the gap is closed. Therefore, it is quite meaningful to apply an early stop to the training process, keeping the useful loss gap for afterward OD methods. [11]

With the following proof, we derive a lower bound for  $\tilde{\Delta}_t^f$ , the loss decreasing speed gap by showing a sufficient condition of  $\tilde{\Delta}_t^f > \epsilon_{lower} > 0$ , which means inlier priority strengthens.

**Assumption 1.** Assume that for each class  $j$ ,  $f^j(\omega_t)$  is  $L - Smooth$ .

**Assumption 2.** At each time  $t$ , there exists a learning rate  $\eta_t > 0$  being sufficiently small to guarantee the decrease of both  $f^i$  and  $f^o$ .

*Proof.* In each iteration, the gradient descent algorithm uses the gradient summed over all samples to update the parameters:

$$\omega^{t+1} = \omega^t - \eta_t \nabla f(\omega_t) \quad (8)$$

Since each  $f^i(\omega_t)$  is  $L - Smooth$ , we have

$$f^i(\omega_{t+1}) = f^i(\omega_t) + \nabla f^i(\omega_t)^T (\omega_{t+1} - \omega_t) \quad (9)$$

$$\begin{aligned} &+ \frac{1}{2} (\omega_{t+1} - \omega_t)^T \nabla^2 f^i(u) (\omega_{t+1} - \omega_t) \\ &\leq f^i(\omega_t) + \nabla f^i(\omega_t)^T (\omega_{t+1} - \omega_t) + \frac{L}{2} \|\omega_{t+1} - \omega_t\|^2, \end{aligned} \quad (10)$$

and

$$\begin{aligned} f^i(\omega_{t+1}) &\geq f^i(\omega_t) + \nabla f^i(\omega_t)^T (\omega_{t+1} - \omega_t) \\ &\quad - \frac{L}{2} \|\omega_{t+1} - \omega_t\|^2, \end{aligned} \quad (11)$$

In (9),  $f(u)$  is some convex combination of  $\omega_{t+1}$  and  $\omega_t$  with respect to multivariate Taylor expansion. We have (10) and (11) by applying Lipschitz smooth, which ensures the term  $(\omega_{t+1} - \omega_t)^T \nabla^2 f(u) (\omega_{t+1} - \omega_t)$  is at most  $L \|\omega_{t+1} - \omega_t\|^2$  and at least  $-L \|\omega_{t+1} - \omega_t\|^2$ . We first focus on the upper bound guaranteed by (10).

$$\begin{aligned} f^i(\omega_{t+1}) &\leq f^i(\omega_t) - \eta_t \nabla f^i(\omega_t)^T \nabla f(\omega_t) + \frac{\eta_t^2 L}{2} \|\nabla f(\omega_t)\|^2 \\ &= f^i(\omega_t) - \eta_t (\|\nabla f^i(\omega_t)\|^2 + \nabla f^i(\omega_t)^T \nabla f^o(\omega_t)) \\ &\quad + \frac{\eta_t^2 L}{2} \|\nabla f^i(\omega_t) + \nabla f^o(\omega_t)\|^2 \end{aligned} \quad (12)$$

From this, we can derive a lower bound of the decreasing speed of averaged loss:

$$\begin{aligned} \frac{1}{|C_i|} (f^i(\omega_t) - f^i(\omega_{t+1})) &\geq \\ &- \frac{\eta_t^2 L}{2|C_i|} (\|\nabla f^i(\omega_t)\|^2 + \|\nabla f^o(\omega_t)\|^2) \\ &+ 2 \cos \theta_t \|\nabla f^i(\omega_t)\| \|\nabla f^o(\omega_t)\| \\ &+ \frac{\eta_t}{|C_i|} (\|\nabla f^i(\omega_t)\|^2 + \nabla f^i(\omega_t)^T \nabla f^o(\omega_t)) \end{aligned} \quad (13)$$

Note that  $\theta_t = \angle(\nabla f^i(\omega_t), \nabla f^o(\omega_t))$ . It can reflect the degree of divergence between the inlier gradients and outlier gradients. A larger  $\theta_t$  means a stronger rival between inliers and outliers, which may drive the model parameters towards two opposite directions respectively. For clarity, we use a simplified notation  $\nabla_i = \|\nabla f^i(\omega_t)\|$ :

$$\begin{aligned} \frac{1}{|C_i|} (f^i(\omega_t) - f^i(\omega_{t+1})) &\geq \\ &- \frac{\eta_t^2 L}{2|C_i|} (\nabla_i^2 + \nabla_o^2 + 2 \cos \theta_t \nabla_i \nabla_o) \\ &+ \frac{\eta_t}{|C_i|} (\nabla_i^2 + \cos \theta_t \nabla_i \nabla_o) \end{aligned} \quad (14)$$

Now we get a lower bound of  $f^i(\omega_t) - f^i(\omega_{t+1})$  with (10). With (11) and a similar procedure, we can derive an upper bound of  $\frac{1}{|C_i|} (f^i(\omega_t) - f^i(\omega_{t+1}))$ :

$$\begin{aligned} \frac{1}{|C_i|} (f^i(\omega_t) - f^i(\omega_{t+1})) &\leq \\ &\frac{\eta_t^2 L}{2|C_i|} (\nabla_i^2 + \nabla_o^2 + 2 \cos \theta_t \nabla_i \nabla_o) \\ &+ \frac{\eta_t}{|C_i|} (\nabla_i^2 + \cos \theta_t \nabla_i \nabla_o) \end{aligned} \quad (15)$$

Note that the previous formulas also apply to the other class  $1 - i$ , since we assume that for each  $l$ ,  $f^l(\omega_t)$  is  $L - Smooth$ . With 2 and the inequation (14), we have:

For each class  $j$ ,

$$\begin{aligned} &-\frac{\eta_t^2 L}{2} (\nabla_j^2 + \nabla_{1-j}^2 + 2 \cos \theta_t \nabla_j \nabla_{1-j}) \\ &\quad + \eta_t (\nabla_j^2 + \cos \theta_t \nabla_j \nabla_{1-j}) > 0 \end{aligned}$$

Hence,

$$\begin{cases} \eta_t L < \frac{2(\min(\nabla_i^2, \nabla_o^2) + \cos \theta_t \nabla_i \nabla_o)}{\nabla_i^2 + 2 \cos \theta_t \nabla_i \nabla_o + \nabla_o^2} \\ \theta_t < \cos^{-1}(-\frac{1}{r}) \end{cases} \quad (16)$$

Now we would like to derive a lower bound for  $\Delta_t^f$  first. From (14) we can infer that a sufficient condition for  $\Delta_t^f > 0$  is:

$$\eta_t (\nabla_i^2 - \nabla_o^2) - \eta_t^2 L (\nabla_i^2 + 2 \cos \theta_t \nabla_i \nabla_o + \nabla_o^2) > 0 \quad (17)$$

Then the sufficient condition for  $\Delta_t^f > 0$  can be written as:

$$\nabla_i^2 - \nabla_o^2 - 2(\min(\nabla_i^2, \nabla_o^2) + \cos \theta_t \nabla_i \nabla_o) \geq 0$$

With  $r_t = \frac{\nabla_i}{\nabla_o}$ , we have 2 cases:  $r_t \geq 1$  and  $r_t < 1$ .

*Case 1,  $r_t \geq 1$ .*

$$\begin{aligned} (r_t^2 - 1)\nabla_o^2 - 2(\nabla_o^2 + 2r_t \cos \theta_t \nabla_o^2) &\geq 0 \\ r_t^2 - 2r_t \cos \theta_t - 3 &\geq 0 \\ r_t &\geq \sqrt{\cos^2 \theta_t + 3} + \cos \theta_t \end{aligned}$$

*Case 2,  $r_t < 1$ .*

$$\begin{aligned} (r_t^2 - 1)\nabla_o^2 - 2(r_t^2 \nabla_o^2 + 2r_t \cos \theta_t \nabla_o^2) &\geq 0 \\ -r_t^2 - 2r_t \cos \theta_t - 1 &\geq 0 \end{aligned}$$

Combining the two cases, we gain a sufficient condition to ensure  $\Delta_t^f > 0$ :

$$r_t \geq \sqrt{\cos^2 \theta_t + 3} + \cos \theta_t \quad (18)$$

Additionally, we also want to inspect the expectation of *sample* loss, i.e.,  $\tilde{\Delta}_t^f$ , instead of the *summed* loss of each class, since sample loss is directly utilized for OD algorithms. With a similar derivation procedure, we can derive a sufficient condition for  $\tilde{\Delta}_t^f > 0$ :

*Case 1,  $r_t \geq 1$ .*

$$|C_o| r_t^2 - 2 \cos \theta_t |C_i| - 2(|C_i| + |C_o|) \geq 0$$

*Case 2,  $r_t < 1$ .*

$$-|C_i| (r_t^2 + 2 \cos \theta_t r_t + 1) \geq 0$$

Combining the two cases, we gain a sufficient condition to ensure  $\tilde{\Delta}_t^f > 0$ :

$$\begin{aligned} r_t &\geq \frac{\cos \theta_t |C_i| + \sqrt{\cos^2 \theta_t |C_i|^2 + 2|C_i||C_o| + |C_o|^2}}{|C_o|} \\ r_t &> \cos \theta_t R + \sqrt{\cos^2 \theta_t R^2 + 2R + 1} \end{aligned} \quad (19)$$

Finally, we gain a sufficient condition that ensures the decreasing speed of sample-wise loss of inlier class  $i$  to be faster than the one of outlier class  $o$ , i.e. inequation (19). Note that,  $\cos \theta_t$  is the divergence metric  $\mathbf{D}(\nabla f^i(\omega_t), \nabla f^o(\omega_t))$ , and  $r_t = \frac{\mathbf{C}(\nabla f^i(\omega_t)) \sum_{x \in C_i} \|\nabla f_x(\omega_t)\|}{\mathbf{C}(\nabla f^o(\omega_t)) \sum_{x \in C_o} \|\nabla f_x(\omega_t)\|}$ , which is the theoretical enlightenment of designing cohesion metric  $\mathbf{C}$  and divergence metric  $\mathbf{D}$ . A larger  $r_t$  ensures a larger lower bound for  $\tilde{\Delta}_t^f > 0$ , indicating a stronger alignment with the OD assumption inlier priority. In current exploratory experiments, the application of these two metrics is heuristic. Intuitively, a larger  $\mathbf{C}(\nabla f^i(\omega_t)) - \mathbf{C}(\nabla f^o(\omega_t))$  indicates a larger  $r_t$ , so  $\mathbf{C}(G_{\text{last}}) - \mathbf{C}(G_{\text{top}})$  is used to approximate  $f^i(\omega_t) - \mathbf{C}(\nabla f^o(\omega_t))$  and as a stopping indicator. We left exploring more elaborate algorithm designs being closer to the theoretical conclusion as our future work.  $\square$

TABLE IV: Hyperparameters of deep UOD models and GradStop

	AE	DeepSVDD	RDP	VAE
#epochs	100			
lr	0.005	0.001	0.5	0.01
k	20	20	20	10
$[t_{C_s}, t_{C_b}]$	[0.01, 0.05]	[0.0, 0.1]	[0, 0.5]	[0.01, 0.5]
$t_{\mathbf{D}}$	1.57	1.57	$\infty$	$\infty$
w	20	10	50	20
$R_{\text{down}}$	0.001			

TABLE V: AEs' performance on individual datasets with  $\text{abs}(\text{improvements}) > 5\%$  among 47 datasets.

Dataset	VanillaAE	AE-G	Improvement
7 Cardiotocography	0.571	0.751	31.39%
28 pendigits	0.769	0.930	20.99%
11 donors	0.707	0.834	17.86%
6 cardio	0.809	0.950	17.43%
23 mammography	0.738	0.846	14.64%
26 optdigits	0.455	0.521	14.59%
8 celeba	0.729	0.834	14.41%
17 InternetAds	0.559	0.615	10.02%
31 satimage-2	0.906	0.990	9.27%
37 Stamps	0.816	0.871	6.74%
35 SpamBase	0.522	0.550	5.43%
15 Hepatitis	0.711	0.745	4.67%
...	...	...	...
1 ALOI	0.568	0.540	-4.99%
12 fault	0.647	0.550	-15.04%

### C. Implementation Details in Experiments

For experiments on AE, RDP, VAE and DeepSVDD and their GradStop versions, we first randomly downsample datasets larger than 10,000 to a size of 10,000 before training to shorten the experiment pipeline. Downsampling almost does not influence the performance evaluation according to our observation. The size of  $B_{\text{eval}}$  is set to 400. For efficiency, we re-sample to generate  $G_{\text{top}}$  and  $G_{\text{last}}$  using GradSample every ten epochs rather than every epoch. To simplify the observation and analysis of training dynamics, we adopted a full-batch gradient descent configuration in the experiments. The training hyperparameter of deep UOD models is in table IV. Other hyperparameters are the same as the default hyperparameters in their original codes. Codes are available at <https://github.com/Yann-zh/gradAE>.

### D. Detailed Experimental Results

We put the performance on individual datasets of AE, DeepSVDD, and their GradStop versions in table V and VI. Due to space limitation, we select datasets on which the absolute improvement in AUC by GradStop is greater than 5%. For RDP and VAE, early stopping does not significantly affect the overall performance.

TABLE VI: DeepSVDD’s performance on individual datasets with  $abs(improvements) > 5\%$  among 47 datasets.

Dataset	DeepSVDD	DeepSVDD-G	Improvement	
36	speech	0.380	0.977	157.33%
7	Cardiotocography	0.409	0.998	143.73%
44	Wilt	0.411	0.913	121.88%
30	satellite	0.439	0.917	108.97%
13	fraud	0.377	0.744	97.52%
4	breastw	0.460	0.883	92.17%
25	musk	0.381	0.727	90.65%
24	mnist	0.503	0.867	72.19%
42	WBC	0.565	0.943	66.84%
31	satimage-2	0.482	0.800	66.04%
19	landsat	0.553	0.893	61.64%
1	ALOI	0.433	0.669	54.50%
33	skin	0.490	0.753	53.57%
9	census	0.524	0.791	50.79%
27	PageBlocks	0.537	0.806	49.94%
20	letter	0.517	0.723	39.76%
16	http	0.490	0.676	37.99%
39	vertebral	0.413	0.530	28.35%
22	magic.gamma	0.537	0.684	27.37%
15	Hepatitis	0.478	0.607	26.83%
21	Lymphography	0.515	0.644	24.90%
45	wine	0.434	0.528	21.83%
43	WDBC	0.498	0.604	21.43%
26	optdigits	0.540	0.634	17.48%
17	InternetAds	0.579	0.667	15.26%
28	pendigits	0.492	0.567	15.23%
46	WPBC	0.475	0.543	14.25%
6	cardio	0.460	0.515	11.88%
23	mammography	0.514	0.554	7.72%
14	glass	0.542	0.581	7.07%
10	cover	0.531	0.563	5.90%
2	annthyroid	0.526	0.555	5.45%
8	celeba	0.499	0.526	5.41%
3	backdoor	0.535	0.555	3.68%
...	...	...	...	...
12	fault	0.622	0.596	-4.23%
5	campaign	0.649	0.611	-5.80%
18	Ionosphere	0.552	0.487	-11.66%
32	shuttle	0.523	0.439	-16.07%
41	Waveform	0.533	0.415	-22.08%
38	thyroid	0.590	0.446	-24.51%
37	Stamps	0.393	0.277	-29.52%

## REFERENCES

- [1] V. Chandola, A. Banerjee, and V. Kumar, “Anomaly detection: A survey,” *ACM computing surveys (CSUR)*, vol. 41, no. 3, pp. 1–58, 2009.
- [2] S. Han, X. Hu, H. Huang, M. Jiang, and Y. Zhao, “Adbench: Anomaly detection benchmark,” *arXiv preprint arXiv:2206.09426*, 2022.
- [3] K.-H. Lai, D. Zha, J. Xu, Y. Zhao, G. Wang, and X. Hu, “Revisiting time series outlier detection: Definitions and benchmarks,” in *Thirty-fifth Conference on Neural Information Processing Systems Datasets and Benchmarks Track (Round 1)*, 2021.
- [4] K. Liu, Y. Dou, Y. Zhao, X. Ding, X. Hu, R. Zhang, K. Ding, C. Chen, H. Peng, K. Shu *et al.*, “Bond: Benchmarking unsupervised outlier node detection on static attributed graphs,” in *Thirty-sixth Conference on Neural Information Processing Systems Datasets and Benchmarks Track*, 2022.
- [5] Y. Dou, Z. Liu, L. Sun, Y. Deng, H. Peng, and P. S. Yu, “Enhancing graph neural network-based fraud detectors against camouflaged fraudsters,” in *Proceedings of the 29th ACM International Conference on Information & Knowledge Management*, 2020, pp. 315–324.
- [6] D. J. Weller-Fahy, B. J. Borghetti, and A. A. Sodemann, “A survey of distance and similarity measures used within network intrusion anomaly detection,” *IEEE Communications Surveys & Tutorials*, vol. 17, no. 1, pp. 70–91, 2014.
- [7] S. Wang, Y. Zeng, X. Liu, E. Zhu, J. Yin, C. Xu, and M. Kloft, “Effective end-to-end unsupervised outlier detection via inlier priority of discriminative network,” *Advances in neural information processing systems*, vol. 32, 2019.
- [8] G. Pang, C. Shen, L. Cao, and A. V. D. Hengel, “Deep learning for anomaly detection: A review,” *ACM Computing Surveys (CSUR)*, vol. 54, no. 2, pp. 1–38, 2021.
- [9] R. Chalapathy and S. Chawla, “Deep learning for anomaly detection: A survey,” *arXiv preprint arXiv:1901.03407*, 2019.
- [10] L. Ruff, J. R. Kauffmann, R. A. Vandermeulen, G. Montavon, W. Samek, M. Kloft, T. G. Dietterich, and K.-R. Müller, “A unifying review of deep and shallow anomaly detection,” *Proceedings of the IEEE*, vol. 109, no. 5, pp. 756–795, 2021.
- [11] Y. Huang, Y. Zhang, L. Wang, F. Zhang, and X. Lin, “Entropystop: Unsupervised deep outlier detection with loss entropy,” in *Proceedings of the 30th ACM SIGKDD Conference on Knowledge Discovery and Data Mining*, 2024.
- [12] L. Ruff, R. Vandermeulen, N. Goernitz, L. Deecke, S. A. Siddiqui, A. Binder, E. Müller, and M. Kloft, “Deep one-class classification,” in *International conference on machine learning*. PMLR, 2018, pp. 4393–4402.
- [13] C. Qiu, T. Pfommer, M. Kloft, S. Mandt, and M. Rudolph, “Neural transformation learning for deep anomaly detection beyond images,” in *International Conference on Machine Learning*. PMLR, 2021, pp. 8703–8714.
- [14] T. Shenkar and L. Wolf, “Anomaly detection for tabular data with internal contrastive learning,” in *International Conference on Learning Representations*, 2021.
- [15] T. Schlegl, P. Seeböck, S. M. Waldstein, U. Schmidt-Erfurth, and G. Langs, “Unsupervised anomaly detection with generative adversarial networks to guide marker discovery,” in *International conference on information processing in medical imaging*. Springer, 2017, pp. 146–157.
- [16] J. Chen, S. Sathe, C. Aggarwal, and D. Turaga, “Outlier detection with autoencoder ensembles,” in *Proceedings of the 2017 SIAM international conference on data mining*. SIAM, 2017, pp. 90–98.
- [17] X. Ding, L. Zhao, and L. Akoglu, “Hyperparameter sensitivity in deep outlier detection analysis and a scalable hyper-ensemble solution,” in *Proceedings of the 36th International Conference on Neural Information Processing Systems*, ser. NIPS ’22, 2024.
- [18] H. Wang, G. Pang, C. Shen, and C. Ma, “Unsupervised representation learning by predicting random distances,” *arXiv preprint arXiv:1912.12186*, 2019.
- [19] C. Zhou and R. C. Paffenroth, “Anomaly detection with robust deep autoencoders,” in *Proceedings of the 23rd ACM SIGKDD international conference on knowledge discovery and data mining*, 2017, pp. 665–674.
- [20] F. T. Liu, K. M. Ting, and Z.-H. Zhou, “Isolation forest,” in *2008 eighth IEEE international conference on data mining*. IEEE, 2008, pp. 413–422.
- [21] Y. Liu, Z. Li, C. Zhou, Y. Jiang, J. Sun, M. Wang, and X. He, “Generative adversarial active learning for unsupervised outlier detection,” *IEEE Transactions on Knowledge and Data Engineering*, vol. 32, no. 8, pp. 1517–1528, 2019.
- [22] Z. Li, Y. Zhao, X. Hu, N. Botta, C. Ionescu, and G. Chen, “Ecod: Unsupervised outlier detection using empirical cumulative distribution functions,” *IEEE Transactions on Knowledge and Data Engineering*, 2022.
- [23] S. Ramaswamy, R. Rastogi, and K. Shim, “Efficient algorithms for mining outliers from large data sets,” in *Proceedings of the 2000 ACM SIGMOD international conference on Management of data*, 2000, pp. 427–438.
- [24] M. M. Breunig, H.-P. Kriegel, R. T. Ng, and J. Sander, “Lof: identifying density-based local outliers,” in *Proceedings of the 2000 ACM SIGMOD international conference on Management of data*, 2000, pp. 93–104.
- [25] C. Qiu, A. Li, M. Kloft, M. Rudolph, and S. Mandt, “Latent outlier exposure for anomaly detection with contaminated data,” in *International Conference on Machine Learning*. PMLR, 2022, pp. 18 153–18 167.
- [26] B. Zong, Q. Song, M. R. Min, W. Cheng, C. Lumezanu, D. Cho, and H. Chen, “Deep autoencoding gaussian mixture model for unsupervised anomaly detection,” in *International conference on learning representations*, 2018.
- [27] Y. Xia, X. Cao, F. Wen, G. Hua, and J. Sun, “Learning discriminative reconstructions for unsupervised outlier removal,” in *Proceedings of the IEEE international conference on computer vision*, 2015, pp. 1511–1519.

- [28] J. Yoon, K. Sohn, C.-L. Li, S. O. Arik, C.-Y. Lee, and T. Pfister, “Self-trained one-class classification for unsupervised anomaly detection,” *arXiv e-prints*, pp. arXiv–2106, 2021.
- [29] N. Morgan and H. Boudlard, “Generalization and parameter estimation in feedforward nets: Some experiments,” in *Advances in Neural Information Processing Systems*, D. Touretzky, Ed., vol. 2. Morgan-Kaufmann, 1989.
- [30] M. Li, M. Soltanolkotabi, and S. Oymak, “Gradient descent with early stopping is provably robust to label noise for overparameterized neural networks,” in *International conference on artificial intelligence and statistics*. PMLR, 2020, pp. 4313–4324.
- [31] Y. Bai, E. Yang, B. Han, Y. Yang, J. Li, Y. Mao, G. Niu, and T. Liu, “Understanding and improving early stopping for learning with noisy labels,” in *Advances in Neural Information Processing Systems*, vol. 34, 2021, pp. 24 392–24 403.
- [32] X. Xia, T. Liu, B. Han, C. Gong, N. Wang, Z. Ge, and Y. Chang, “Robust early-learning: Hindering the memorization of noisy labels,” in *International conference on learning representations*, 2020.
- [33] D. Arpit, S. Jastrzebski, N. Ballas, D. Krueger, E. Bengio, M. S. Kanwal, T. Maharaj, A. Fischer, A. Courville, Y. Bengio *et al.*, “A closer look at memorization in deep networks,” in *International conference on machine learning*. PMLR, 2017, pp. 233–242.
- [34] D. M. Hawkins, *Identification of outliers*. Springer, 1980, vol. 11.
- [35] A. P. Bradley, “The use of the area under the roc curve in the evaluation of machine learning algorithms,” *Pattern recognition*, vol. 30, no. 7, pp. 1145–1159, 1997.
- [36] E. Franczi, M. Baity-Jesi, and A. Lucchi, “A theoretical analysis of the learning dynamics under class imbalance,” in *Proceedings of the 40th International Conference on Machine Learning*, ser. Proceedings of Machine Learning Research, A. Krause, E. Brunskill, K. Cho, B. Engelhardt, S. Sabato, and J. Scarlett, Eds., vol. 202. PMLR, 2023, pp. 10 285–10 322.
- [37] R. Kiani, W. Jin, and V. S. Sheng, “Survey on extreme learning machines for outlier detection,” *Mach. Learn.*, 2024.
- [38] Z. He, X. Xu, and S. Deng, “Discovering cluster-based local outliers,” *Pattern Recogn. Lett.*, vol. 24, no. 9–10, p. 1641–1650, 2003.
- [39] D. P. Kingma and M. Welling, “Auto-encoding variational bayes,” 2022. [Online]. Available: <https://arxiv.org/abs/1312.6114>
- [40] M. Jiang, S. Han, and H. Huang, “Anomaly detection with score distribution discrimination,” in *Proceedings of the 29th ACM SIGKDD Conference on Knowledge Discovery and Data Mining*, ser. KDD ’23, 2023.